ANATOMIA HISTOLOGIA EMBRYOLOGIA
JOURNAL OF VETERINARY MEDICINE
Anatomia, Histologia, Embryologia

ORIGINAL ARTICLE

# Microstructure and Hardness of Buffalo's Hoofs

B. M. Assis[1], L. A. F. Silva[2], C. R.O. Lima[3], R. F. Gouveia[4], V. A. S. Vulcani[1], F. J. F. de Sant'Ana[5]* and R. E. Rabelo[1]

Addresses of authors: [1] Universidade Federal de Goiás, Regional Jataí, Jataí, GO, Brazil;
[2] Escola de Veterinária e Zootecnia, Universidade Federal de Goiás, Goiânia, GO, Brazil;
[3] Universidade Estadual de Goiás, Campus Jataí, Jataí, GO, Brazil;
[4] Laboratório de Nanotecnologia Nacional, Centro Nacional para Energia e Materiais, Campinas, SP, Brazil;
[5] Laboratório de Diagnóstico Patológico Veterinário, Universidade de Brasília, Brasília, DF, Brazil

***Correspondence:**
Tel.: +55 61 3468 7255;
fax: +55 61 3468 7255;
e-mail: santanafjf@yahoo.com

With 1 figure and 2 tables

Received February 2017; accepted for publication June 2017

doi: 10.1111/ahe.12288

## Summary

The aim of this study was to describe the microstructure of hoof capsules of the buffalo. In addition, the study emphasized the morphometric aspects of the horn tubules, the Vickers nanohardness of the dorsal and abaxial walls and sole of the digits of the thoracic and pelvic limbs of the buffalo. The abaxial wall in the thoracic and pelvic digits showed larger diameter of the horn tubules when compared to all dorsal wall and sole. In addition, the abaxial wall of the thoracic digits showed larger diameter of the horn tubules when compared with the pelvic digits. According to the three-dimensional microtomography, the dorsal wall was higher in density compared with the abaxial wall. The latter exhibited an intermediate density, while the sole showed the lowest density. The Vickers nanohardness test showed that there was no difference in hardness and resistance between the experienced regions. However, the elastic modulus was greater on the transversal section of the hoof capsule. In conclusion, the results of the current study show that modern technologies such as microtomography and subsequent imaging can be used to investigate details of the basic morphology in different regions of the buffalo's hoof.

## Introduction

Due to the low rate of occurrence of foot diseases in buffalo, evaluating the microstructure of the hoof capsule in this species may represent an innovation in bovine podology research (Hussni et al., 2009). The hoof capsule is composed of keratinized epidermal tissue, which is, divided into perioplic segment, coronary segment, wall segment, sole segment and bulb. Coronary and wall segment are connected with the sole segment by the white line (Greenough, 2007). The epidermis of the hoof capsule is responsible for the proliferation of keratinocytes and keratin synthesis, maintaining the quality and integrity of hoof areas (König and Liebich, 2004). Concentric compaction of tubular keratin forms tubular structures, except in the wall segment of the modified epidermis (Banks, 1991). Studies had shown that the density, types and number of tubules connected through disulphide bridges and intercellular cement directly affects the resistance and hardness of this anatomical structure (Tomlinson et al., 2004). In this way, addressed scientific studies in this topic are still limited.

Two-dimensional (2D) and three-dimensional (3D) microtomography and the nanohardness test are important tools in geology, mechanical and civil engineering (Lima et al., 2009), aeronautics (Girodin, 2008), dentistry and orthopaedics (Silva, 2012) and petrography (Lopes et al., 2012). These tests comprise cutting-edge technology and high-specificity assays. However, there is a lack of information on the hoof microstructure, hardness and hoof capsule resistance in buffalo and other ruminants. (Rabelo et al., 2015) Two-dimensional microtomography allows the evaluation of the microstructure, which using X-ray attenuation differences makes possible the estimative of the density variation of the material. Thus, it is possible to differentiate the density of the analysed

material based on a colorimetric scale using DataViewer® software. Two-dimensional microtomography also allows the detailed examination of the material's behaviour and the quantification of certain components of their structure using the CTvox®, CTan® and CTvol® (Bruker Corporation, Kontich, Belgium) software packages. The Vickers nanohardness test measures the resistance to penetration or the resistance to deformation of a particular material in real time. The values of applied force and depth penetration generate a characteristic curve containing information about the elastic and plastic properties of the analysed material, which indicate the Vickers hardness and the elastic modulus.

This study describes the microstructure of the hoof capsule, with emphasis on the morphometric aspects of the horn tubules and Vickers nanohardness of the hoof's dorsal wall, abaxial wall and the sole of the hoof capsule of the thoracic and pelvic limbs of buffalo.

## Materials and Methods

The study was carried out after approval of the project by the Ethics Committee on Animal Use, UFG-Pro-Rectory of Research and Innovation (CEUA-PRPI-UFG), protocol no. 20/2014.

Fifty-six fresh hoof capsules, distributed evenly between the thoracic and pelvic limbs, were sampled from seven adult Jafarabadi buffalo cows, ageing from 24 to 60 months old. The collected material corresponded to 28 digits identified as lateral pelvic and 28 digits as medial thoracic. These digits were chosen because they are subjected to a greater weight load in bi-ungulate ruminants, including buffalo, and in cattle these digits exhibit a higher incidence of lesions and foot diseases (Tomlinson et al., 2004). Sample fragments measuring $10 \times 10$ mm were collected in duplicated samples, one in the horizontal direction and one transversal in relation to the hoof's keratinized tissue at the dorsal wall, abaxial wall and pre-bulbar sole in the medial third of the medial digits of the thoracic limbs and the lateral digits of the pelvic limbs. For the 2D and 3D microtomography and Vickers nanohardness evaluations, the sampled material was prepared, ensuring the removal of soft tissue and dirt, and then placed in plastic containers, which were labelled and frozen at −15°C (Rabelo et al., 2015). For the analysis purposes of 2D and 3D microtomography and nanohardness test, the samples were previously thawed at room temperature.

The 2D and 3D microtomography evaluations were performed using a SkyScan 1272® microtomograph (Bruker Corporation): source voltage (kV) = 25, source current ($\mu$a) = 180, number of rows = 820, number of columns = 1224, scaled image pixel size ($\mu$m) = 17, filter = Al 0.25 mm [5–7]. DataViewer® was employed for 2D evaluations, and CTvox®, CTan® and CTvol® (Bruker) for 3D evaluations. The 2D samples were assessed by interpreting the colorimetric scale produced by the above-mentioned software. The colour scale ranged from dark brown to light green, according to the regions that showed lower or greater hardness, respectively.

The specimens selected for this assessment were embedded in polymer resin, T208 resin (Cristal®), styrene monomers, the MEK TGDM50 catalyst and dimethylamine at appropriate ratios to achieve hardening in approximately 3 min, aiming the verification of sample's stability. Initially, the fragments were placed in 5 cm diameter aluminium cylinders, and the resin was added over each sample. After drying the material, surface wear was applied using 80–2500 grit wet sandpaper (Arotec Polisher – Aropol E®, Teclago Indústria e Comércio Ltda, Vargem Grande Paulista, Brazil) until the hoof fragments embedded in the resin were exposed. At the end, the cylinder was removed, and the prepared samples were analysed using a PB1000® Mechanical Tester (Nanovea, Irvine, CA, USA), that performs nanohardness test, according to Fischer-Cripps (2011). The result of the nanohardness test shows the vickers hardness and the elastic modulus of the analysed samples.

To analyse the results, the *t*-test was used to compare two means, and analysis of variance (ANOVA) was used to compare three means at a 5% significance level, according to Sampaio (2010).

## Results

The 2D and 3D microtomography analyses revealed important aspects of the structural organization of the hoof tissue that composes the keratinized epidermis in buffalo. The various regions of the hoof capsule were visualized by X-ray imaging, suggesting differences in the density, resistance and hardness of the keratinized epidermis based on the colorimetric scale (Fig. 1a,b).

In the 2D microtomography assessment, the dorsal wall region exhibited a predominance of blue, pink and light green colours, suggesting a higher density. The abaxial wall showed a predominance of blue, pink and yellow, indicating an intermediate density. The sole displayed a predominance of yellow, pink and brown, indicating an anatomical region with lower density (Fig. 1c–e).

The intratubular and extratubular keratin of the hoof capsules are connected through the disulphide bridges in a concentric shape, with the intratubular presenting a lower density than the extratubular (Fig. 1f–h). The Two-dimensional microtomography enabled the confirmation of the absence of pores in the hoof capsule (Fig. 1f–h), which is an anatomical structure formed exclusively by

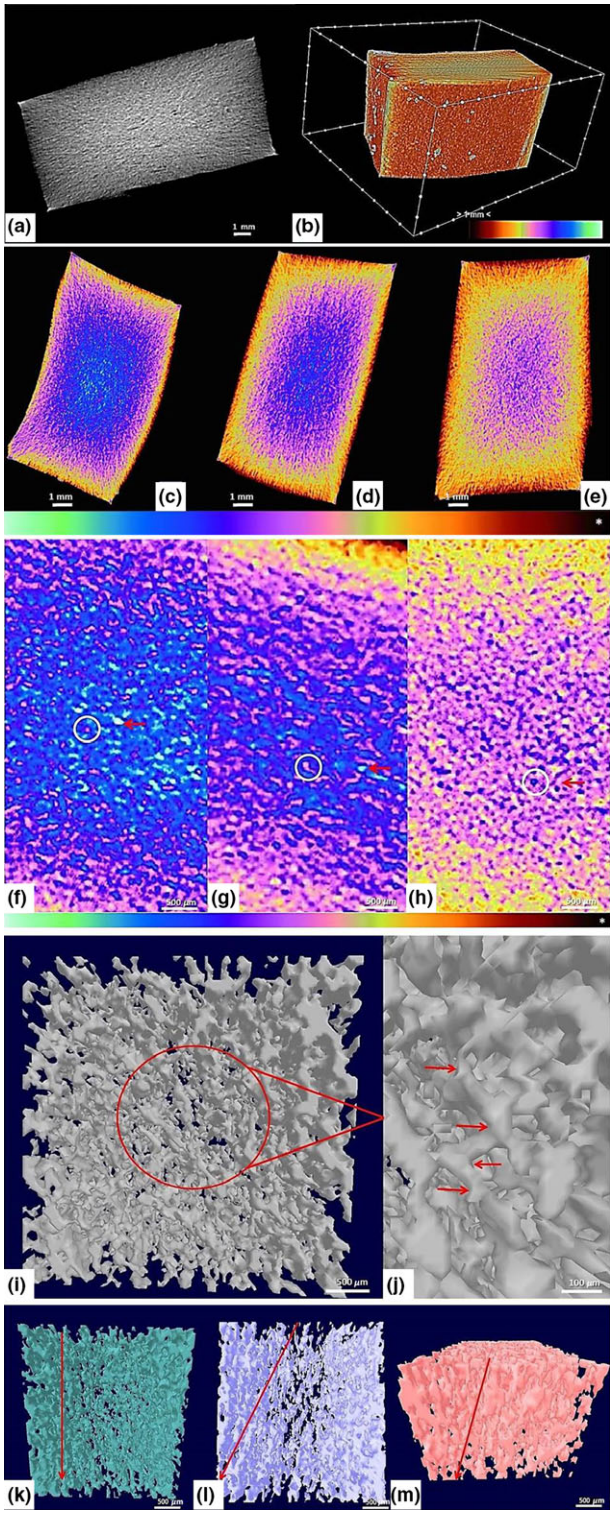


Fig. 1. Structural organization of hoof tissue constituting the keratinized epidermis of buffalo hoof. (a) Two-dimensional microtomography of the dorsal wall of the hoof capsule. (b) Three-dimensional reconstruction of the dorsal wall of the hoof capsule and the colorimetric scale that allows differences in the density to be assessed based on X-ray attenuation (brown and yellow colour represent the regions of lower densities and the colours blue and light green to the regions of bigger density). Two-dimensional microtomography images of buffalo hoof capsule. (c) Dorsal wall of the hoof capsule. Note the predominance of blue, pink and light green, representing a region with higher density. (d) Abaxial wall of the hoof capsule with a predominance of blue, pink and yellow, representing a region with intermediate density. (e) The sole shows a predominance of yellow, pink and brown, indicating a region with a lower density. The white asterisk (*) represents the colorimetric scale. Two-dimensional microtomography of buffalo hoof capsule. (f and g) Note the dorsal and abaxial walls of the hoof capsule, respectively, showing pink intratubular keratin (white circle) and blue and light green extratubular keratin (red arrow), indicating that intratubular keratin shows a lower density than extratubular keratin. (h) On the sole of the hoof, intratubular keratin is blue (white circle), and extratubular keratin is pink (red arrow), indicating a higher density of intratubular keratin compared with extratubular keratin. The white asterisk (*) indicates the colorimetric scale. Three-dimensional microtomography (3D model obtained on CTvol) of the hoof capsule of buffalo digits. (i) Intratubular keratin in the dorsal wall region. (j) Horn tubules arranged in a concentric helical shape, as indicated by the red arrows. Microtomography images of the hoof capsule of the buffalo digits, indicating the angle of the horn tubules. (k) A 90° angle (red arrow) and (l) a 65° angle (red arrow), both in relation to the coronary corium. (m) The horn tubules are at a 70° angle (red arrow) in relation to the laminar corium.

horn tubules (Fig. 1i,j). In the dorsal and abaxial wall, intratubular keratin was identified as a pinkish colour, while extratubular keratin was coloured blue and light green. The hoof sole exhibited exactly the opposite displaying blue intratubular keratin and pink extratubular keratin. In this case, both keratin types showed a density that was inversely proportional to the hardness of the abaxial and dorsal walls, by the inversion of colours that are identified in the colorimetric scale.

In addition, 3D microtomography revealed horn tubules seemed to be arranged in parallel to each other, organized in a concentric helical shape in all regions of the hoof capsule (Fig. 1i,j), which is a characteristic that may increase the hardness of the hoof capsule of this species.

The 3D microtomography analysis also enabled the observation that in each region of the hoof capsule, the horn tubules exhibit different angles in relation to the coronary corium (Fig. 1k–m). With regard to the papillae of the coronary corium, the horn tubules of the dorsal and abaxial wall are arranged at a 90° and a 65° angle, respectively. Related to the sole's horn tubules were verified an angle approximately 70° in relation to the perioplic segment.

Using 3D microtomography, it was possible to measure the diameter of the horn tubules and their respective percentages in each region of the hoof capsule. It also allowed the quantification of the exact number of these structures in different points of the hoof. Furthermore,

the 3D microtomography enabled the comparison of the diameter and amount of horn tubules present in the dorsal and abaxial wall and hoof sole in both medial and lateral digits of the thoracic and pelvic limbs (Table 1).

Regarding Vickers nanohardness, the results shown for the hoof capsule can be seen in Table 2, which considers the medial and lateral digits of both thoracic and pelvic limbs and the hoof, dorsal and abaxial wall and sole regions. Based on these results, it was possible to compare the Vickers hardness and elastic modulus of the abovementioned regions in both medial and lateral hoof capsules of the thoracic and pelvic limbs. It also allowed the observation that the assessed elastic modulus in the transversal cut of the horn tubules presented to be greater when compared to the horizontal cut.

## Discussion

The differences of density between the dorsal wall, the abaxial wall and sole may be related to the variation in hardness and resistance of these structures. Previous studies (Budras et al., 1996; Tomlinson et al., 2004) attributed the differences in hardness among the hoof regions of cattle to the greater body weight load on the dorsal and abaxial walls compared to the sole. Therefore, the present findings do not represent a unique characteristic of buffalo.

The results of the present study suggest that microtomography is a thorough and accurate method for measuring X-ray attenuation, which is correlated with density in different regions of the buffalo's hoof. The difference in hardness in a decreasing order, starting from the dorsal and abaxial wall until the sole, can be also related to have a connection with the structure of extratubular and intratubular keratin. Initially, the greater hardness of the wall compared to the sole may be related to a greater body weight load, as these animals support their weight using the hoof wall (Greenough, 2007; Basurto et al., 2008). However, further studies are required to explain the inverse hardness pattern exhibited by the intratubular and extratubular keratin of the sole. According to the literature (Budras et al., 1996; Tomlinson et al., 2004; Tombolato et al., 2010), this inverse pattern may be attributed to the fact that the sole carries out the function of impact absorption and therefore shows greater softness.

Although citations have not been found in literature (Tomlinson et al., 2004; Mulling and Hagen, 2012), it is considered that the lack of pores in the horn capsule of buffalo which was verified in this study, can actually provide greater hardness and resistance to the hoof of the referred animal. Under these circumstances, hooves become more resistant to the development of foot lesions and injuries when compared to other ruminants. It is further believed that an absence of pores decreases the water content of the hoof capsules, at the same time the porous tissues became higher and consequently makes the tissue more fragile (Franck et al., 2006).

Table 1. Diameter, percentage and total number of horn tubules in buffalo digits analysed using 3D microtomography

| | Percentage of horn tubules (%) | | | | | |
|---|---|---|---|---|---|---|
| DIG/HR/AS Diameter | 17 $\mu$m | 51 $\mu$m | 85 $\mu$m | 119 $\mu$m | 153 $\mu$m | No. TB/mm$^2$ |
| TL-medial | 37.23 ± 9.46a | 49.16 ± 2.16a | 10.85 ± 7.17a | 2.56 ± 0.97a | 0.03 ± 0.01a | 30.03 ± 3.51a |
| PL-lateral | 43.25 ± 2.48a | 50.34 ± 0.66a | 6.06 ± 0.43a | 0.35 ± 0.34b | 0.00 ± 0.00a | 28.72 ± 1.83a |
| TL-DW | 42.36 ± 0.95a | 49.63 ± 1.23a | 7.58 ± 2.69b | 0.42 ± 0.026b | 0.00 ± 0.00a | 25.80 ± 2.48a |
| TL-ABW | 26.31 ± 1.67b | 46.84 ± 1.56a | 19.07 ± 3.25a | 7.14 ± 1.45a | 0.10 ± 0.00a | 36.72 ± 5.75a |
| TL-SOL | 43.01 ± 1.41a | 50.99 ± 1.80a | 5.88 ± 2.12b | 0.11 ± 0.01b | 0.00 ± 0.00a | 27.98 ± 2.55a |
| PL-DW | 45.84 ± 2.34a | 49.67 ± 1.65a | 4.29 ± 1.23ab | 0.12 ± 0.002a | 0.00 ± 0.00a | 27.35 ± 2.36a |
| PL-ABW | 40.89 ± 0.85a | 50.35 ± 2.97a | 8.07 ± 2.45a | 0.74 ± 0.03a | 0.00 ± 0.00a | 30.80 ± 2.45a |
| PL-SOL | 46.51 ± 2.66a | 50.72 ± 1.76a | 2.76 ± 0.06b | 0.00 ± 0.00a | 0.00 ± 0.00a | 30.14 ± 2.67a |
| TL-ABW | 26.31 ± 1.67b | 46.84 ± 1.89a | 19.07 ± 3.25a | 7.14 ± 1.45a | 0.10 ± 0.01a | 36.72 ± 5.75a |
| PL-ABW | 40.89 ± 0.85a | 50.35 ± 2.97a | 8.07 ± 2.45b | 0.74 ± 0.03b | 0.00 ± 0.00a | 30.80 ± 2.45a |
| TL-DW | 42.36 ± 0.95a | 49.63 ± 1.23a | 7.58 ± 2.69a | 0.42 ± 0.026a | 0.00 ± 0.00a | 25.80 ± 2.48a |
| PL-DW | 45.84 ± 2.34a | 49.67 ± 1.65a | 4.29 ± 1.23a | 0.12 ± 0.002a | 0.00 ± 0.00a | 27.35 ± 2.36a |
| TL-SOL | 43.01 ± 1.41a | 50.99 ± 1.80a | 5.88 ± 2.12a | 0.11 ± 0.001a | 0.00 ± 0.00a | 27.98 ± 2.55a |
| PL-SOL | 46.51 ± 2.66a | 50.72 ± 1.76a | 2.76 ± 0.06a | 0.00 ± 0.00a | 0.00 ± 0.00a | 30.14 ± 2.67a |
| Mean | 40.24 | 49.75 | 8.46 | 1.45 | 0.03 | 29.56 |

DIG, digits; HR, hoof region; AS, anatomical site; LD, lateral digit; MD, medial digit; TL, thoracic limb; PL, pelvic limb; TL, thoracic limb; PL, pelvic limb; DW, dorsal wall; ABW, abaxial wall; SOL, sole; No. TB/mm$^2$, number of horn tubules per mm$^2$. Means followed by different letters in the same column for the same variable differ from each other significantly ($P < 0.05$). Means followed by same letters in the same column for the same variable do not differ from each other significantly ($P > 0.05$).

Table 2. Vickers nanohardness and elastic modulus values for the hoof capsule of buffalo digits

| DIG/HR/AS | Vickers nanohardness | Elastic modulus |
|---|---|---|
| TL | 25.37 ± 3.31a | 4.57 ± 0.36b |
| PL | 26.28 ± 2.95a | 4.50 ± 0.32b |
| DW | 26.55 ± 4.08a | 4.50 ± 0.22b |
| ABW | 26.19 ± 2.42a | 4.75 ± 0.38b |
| SOL | 24.46 ± 2.60a | 4.71 ± 0.40b |
| TL-DW | 25.31 ± 4.20a | 4.47 ± 0.19b |
| TL-ABW | 26.50 ± 2.38a | 4.64 ± 0.28b |
| TL-SOL | 24.28 ± 3.32a | 4.86 ± 0.37b |
| PL-DW | 28.45 ± 4.12a | 4.54 ± 0.28b |
| PL-ABW | 25.61 ± 1.56a | 4.90 ± 0.49b |
| PL-SOL | 24.55 ± 1.45a | 4.48 ± 0.35b |
| TL-MD | 24.32 ± 3.10a | 4.45 ± 0.40b |
| TL-LD | 26.40 ± 3.35a | 4.75 ± 0.27b |
| PL-MD | 25.39 ± 3.37a | 4.50 ± 0.31b |
| PL-LD | 27.18 ± 2.42a | 4.67 ± 0.51b |
| TL-LD | 26.40 ± 3.35a | 4.75 ± 0.27b |
| PL-LD | 27.18 ± 2.42a | 4.67 ± 0.51b |
| TL-MD | 24.32 ± 3.10a | 4.45 ± 0.40b |
| PL-MD | 25.39 ± 3.37a | 4.50 ± 0.31b |
| CS | 26.07 ± 4.66a | 5.12 ± 0.12a |
| LS | 26.42 ± 3.19a | 4.57 ± 0.20b |
| Mean | 25.74 | 4.65 |

LD, lateral digit; MD, medial digit; TL, thoracic limb; PL, pelvic limb; DW, dorsal wall; ABW, abaxial wall; SOL, sole; CS, cross-section; LS, longitudinal section. Means followed by the same letters in the same column do not differ significantly ($P > 0.05$). Means followed by different letters in the same column differ from each other significantly ($P < 0.05$).

Franck et al. (2006), when studying the cattle hoof observed three layers of horn tubes in the abaxial wall of the hoof capsule. The first region presented absence of tubules, the second showed oval tubules and the third was with tubules of greater diameter and elliptical shape. However, these authors did not observe the helical shape of the tubules as revealed in the current study. Differently from the corneal tubules of the hoof capsule, Kasapi and Gosline (1997) reported that the hooves of horses have six layers of different horn tubes, with differing diameters and orientation of the keratin filaments. Another striking difference found in this species is that the medullary region of the corneal tubules is linear and surrounded by up to nine layers of cortical cells called lamellae. These lamellae are concentric, helical and arranged at different angles. This complex feature in the microstructures of the corneal tubules of horses seems to be related to the better distribution of force inside the hull to prevent fractures reaching its interior.

In cattle and buffalo, the force distribution does not occur equally within the hoof, as described by Van der Tol et al. (2002). These authors state that the horn cases that suffer the greatest wear stress when walking are the thoracic and lateral pelvic medial digits. In these digits, the centre of pressure inside the hoof (Cop) moves palmary to dorsal direction with greater pressure on the sole and then to the wall. Van der Tol et al. (2002) further states that the region where there is greater mechanical stress is more susceptible to injury. In horses, support to the ground is lateral–medial and the hoof (Cop) also moves palmary to dorsal direction, but the higher pressure moves from the centre of the hoof to the wall (Kasapi and Gosline, 1997; Van Heel et al., 2004). Although some characteristics of cattle and buffalo's hooves have been elucidated, additional studies are needed.

However, microstructural analyses were performed in equine and bovine hooves (Mckittrick et al., 2012), even though, it was not taken into deeper discussion. Thus, based on the previous findings (Tombolato et al., 2010), it is suggested that the concentric helical shape of horn tubules must be related to the keratin intratubular arrangement, which forms alpha-keratin, the main constituting protein of keratinized epidermis. In keratinized tissues of non-mammalian animals such as a bird feather and reptile skin, a keratin is found in the form of pleated sheet (beta-keratin; Gupta and Ramnani, 2006).

By analysing the 3D microtomography, another significant finding included the angulation difference of the horn tubules in distinct regions of hoof capsule, which has not yet been investigated in the specialized literature (Tombolato et al., 2010; Mckittrick et al., 2012). The greatest angle identified on the dorsal wall, followed by the sole and abaxial wall with the smallest angle, have not been analysed. However, it is believed that the horn tubules inclination follows the horn capsule growth direction. Nevertheless, further studies are needed to compare this finding to the hoof hardness. It is possible by comparing buffalo to different cattle breeds. Considering the percentage and total number of horn tubules, it was verified that thoracic limbs presented a greater diameter, percentage and total number of tubules compared to the pelvic limbs. This finding must be related to the greater body weight load on the thoracic limbs (Tomlinson et al., 2004). Previous studies in cattle (Budras et al., 1996; Tomlinson et al., 2004) have obtained similar results those described in the current investigation.

It is believed that the abaxial wall of the thoracic medial digits has undergone a functional adaptation to support more weight. Previous studies (Greenough, 2007; Tombolato et al., 2010) demonstrated that the abaxial wall receives a greater weight load, which may lead to increased keratin deposition. The abaxial wall of the pelvic lateral digits exhibited a higher percentage and total number of horn tubules. Furthermore, it was noted greater angles with a larger diameter compared to the

dorsal wall and sole of the same digits. These findings are believed to be justified by the fact that this anatomical region receives a higher animal weight load compared to the abaxial wall medial digits of pelvic limbs.

Studies conducted in cattle (Schaller, 1999; König and Liebich, 2004; Greenough, 2007) pointed that medial digits of the thoracic limbs bear a greater body weight load; therefore, the results in the present study agree with the findings of the above-mentioned studies. Due to this particularity, it is suggested that increased keratin deposition occurs in the digits of the thoracic limbs and consequently, they exhibit horn tubules with larger diameters.

By considering the results, there is no available explanation for the lack of differences in the total number of horn tubules per $mm^2$ in those different analysed regions in the digits of thoracic and pelvic limbs. In contrast, studies conducted recently in cattle and in horses (Basurto et al., 2008; Tombolato et al., 2010), suggest that a greater number of horn tubules in the hoof capsule can confer higher resistance; however, these researchers did not investigate the analysed regions. Due to the complexity of the subject, there is a need of additional studies to better clarify this finding. In addition, a comparison is needed between the hoof capsules of the digits of healthy animals with animals affected by foot diseases, deficiency diseases or even among species.

By utilizing cattle and antelope horns, Abdullahi et al. (2014) found that the nanoindentation technique indicated that the horn capsule exhibits greater Vickers hardness at the skull base, which increases until the middle portion of the horn and then gradually decreases from this segment to its apical portion. Based on these findings, it is believed that the lack of differences related to the hardness Vickers level in many different hoof capsule regions in buffalo is likely related to the standardization of the sample gathering location, which was performed in the medial third of each digit.

Furthermore, there were significant statistic differences in the elastic modulus by considering the Vickers nanohardness test. This modulus showed, however, greater expressions when compared to the longitudinal sections. This result could be explained by considering that, there is a greater elasticity in hoof capsule regions in the transverse direction, as the horn tubules require higher flexibility due to the greater body weight load imposed on this structure.

Regarding the difference in density of the various horn capsules regions of buffalo, this characteristic is believed to be directly related to the resistance and hardness of the involved structures. This study shows that the differences in Vickers hardness of horn capsule regions in the bubaline digits have not been found. Nonetheless, the elastic modulus was greater on the transversal section of the horn capsule in relation to direction of the horn tubules once compared with the longitudinal section. Besides, this characteristic provides to the horn capsule, a biomechanical performance similar to a mechanism that expands under an exerted pressure by the animal's body weight load, and after retracts when the pressure is taken off.

## Acknowledgements

This work was supported by grants of CNPq – National Council for Scientific and Technological Development (Process: 449753/2014-0) and Fapeg – Research Support Foundation of the State of Goiás (Process: 20122012267001141) Research supported by LNNano – Brazilian Nanotechnology National Laboratory, CNPEM/MCTIC. LMN – Nanoestructured Materials Laboratory, PO Box 6192, 13083-970, Campinas, SP, Brazil.

## References

Abdullahi, U., A. Salihi, and A. B. Ali, 2014: Hardness behaviour of thermoplastic cattle horn using nanoindentation technique. Asian J. Eng. Technol. **2**, 169–173.

Banks, W. J., 1991: Histologia Veterinária Aplicada, 2nd edn. São Paulo: Manole.

Basurto, R. N., L. S. Arrieta, H. V. Castrejón, J. A. E. Martínez, and C. A. C. Herrera, 2008: Effect of zinc methionine on the equine hoof: an evaluation by environmental scanning electron microscopy. Vet. Mexico **39**, 247–251.

Budras, K. D., C. Mulling, and A. Horowitz, 1996: Rate of keratinization of the wall segment of the hoof and its relation to width and structure of the zona alba (white line) with respect to claw disease in catlle. Am. J. Vet. Res. **57**, 444–455.

Fischer-Cripps, A. C., 2011: Nanoindentation – Hardcover. New York, NY: Springer International Publishing.

Franck, A., G. Cocquyt, P. Simoens, and N. De Belie, 2006: Biomechanical properties of bovine Claw horn. Biosys. Eng. **93**, 459–467.

Girodin, D., 2008: Deep nitrided 32CrMoV13 steel for aerospace bearings applications. technical review paper. SNR element. Bearing Technol. **16**, 24–31.

Greenough, P. R., 2007: Bovine Laminitis and Lameness - A Hands on Approach. Philadelphia, PA: Sounders Elsevier.

Gupta, R., and P. Ramnani, 2006: Microbial keratinases and their prospective applications: an overview. Appl. Microbiol. Biotecnol. **70**, 21–33.

Hussni, C. A., R. C. Veronezi, A. L. G. Alves, J. L. M. Nicolett, A. Thomassian, and L. C. Vulcano, 2009: Fresamento da falange distal como tratamento de osteíte em bubalino: Relato de caso. Continuous Educ. J. CRMV-SP **5**, 87–93.

Kasapi, M. A., and J. M. Gosline, 1997: Design complexity and fracture control in the equine hoof wall. J. Exp. Biol. **200**, 1639–1659.

König, H. E., and H. Liebich, 2004: Veterinary Anatomy of Domestic Animals, 4th edn. Stuttgart: Schattauer GmbH. pp. 70-99.

Lima, I., R. T. Lopes, L. F. Oliveira, and J. M. Alves, 2009: Análise de estrutura óssea através de microtomografia computadorizada 3D. Rev. Bras. Fís. Méd. **2**, 6–10.

Lopes, A. P., A. P. Fiori, J. M. Reis Neto, C. Marchese, E. M. G. Vasconcellos, B. Trzascos, C. T. Onishi, C. V. Pinto-Coelho, R. Secchi, and G. F. Silva, 2012: Análise tridimensional de rochas por meio de microtomografia computadorizada de raios-x integrada a petrografia. Geociências. **31**, 129–142.

Mckittrick, J., P. Y. Chen, S. G. Bodde, W. Yang, E. E. Novitskaya, and M. A. Meyers, 2012: The structure, functions and mechanical properties of keratin. J. Material. **64**, 331–342.

Mulling, C., and J. Hagen, 2012: Importance of claw disorders and functional anatomy of the claw. Prakt. Tierarzt. **93**, 4–10.

Rabelo, R. E., V. A. S. Vulcani, F. J. F. Sant'Ana, L. A. F. Silva, B. M. Assis, and G. H. M. Araújo, 2015: Microstructure of Holstein and Gir breed adult bovine hooves: histomorphometry, three-dimensional microtomography and microhardness test evaluation. Arq. Bras. Med. Vet. Zootec. **67**, 1492–1500.

Sampaio, I. B. M., 2010: Estatística Aplicada à Experimentação Animal, 3rd edn. Belo Horizonte: FEP-MVZ.

Schaller, O. 1999: Nomenclatura Anatômica Veterinária Ilustrada. São Paulo: Manole.

Silva, A. M. H., 2012: Análise microestrutural óssea trabecular utilizando microtomografia computadorizada tridimensional. Master of Science thesis, Universidade de São Paulo, São Carlos, SP.

Tombolato, L., E. E. Novitskaya, P. Y. Chen, F. A. Sheppard, and J. Mckittrick, 2010: Microstructure, elastic properties and deformation mechanisms of horn keratin. Acta Biomater. **6**, 319–330.

Tomlinson, D. J., C. H. Mulling, and T. M. Fakler, 2004: Formation of keratins in the bovine claw: roles of hormones, minerals, and vitamins in functional claw integrity. J. Dairy Sci. **87**, 797–809.

Van der Tol, P. P. J., J. H. M. Metz, E. N. Noordhuizen-Stassen, W. Back, L. C. R. Braam, and W. A. Weijs, 2002: The pressure distribution under the bovine claw during square standing on a flat substrate. J. Dairy Sci. **85**, 1476–1481.

Van Heel, M. C. V., A. Barneveld, P. R. Van Weeren, and W. Back, 2004: Dynamic pressure measurements for the detailed study of hoof balance: the effect of trimming. Equine Vet. J. **36**, 778–782.